Chemistry–A European Journal
Research Article
doi.org/10.1002/chem.202302552
Chemistry Europe
European Chemical Societies Publishing
www.chemeurj.org

Hole-Transporting Materials based on Oligo(hetero)aryls with a Naphthodithiophene Core – Succinct Synthesis by Twofold Direct C–H Olefination

Chia-Chi Hsu[+],[a] Kun-Mu Lee[+],[b, c] Xiao-Wei Wu,[a] Li Lin,[a] Wei-Lun Yu,[a] and Ching-Yuan Liu*[a]

This work demonstrated the first synthetic application of direct C–H olefinations in the step-saving preparation of various hole-transporting materials (HTM) for efficient perovskite solar cells (PSC). Cross-dehydrogenative couplings of naphthodithiophene (NDT) with vinyl arenes under palladium-catalysis facilely generated various new oligo(hetero)aryls with internal alkenes. Reaction conditions were optimized, which gave the product isolated yields of up to 71% with high (*E*)-stereoselectivity. These readily accessible NDT core-based small molecules involving olefin as π-spacers displayed immediate power conversion efficiencies of up to 17.2% without a device oxidation process that is required for the commercially available **spiro-OMeTAD** and most other existing HTMs while fabricated in corresponding PSC devices.

Introduction

Construction of carbon-carbon bonds via direct C–H activations has been attracting considerable research interests for past few decades.[1–8] Numerous pioneering synthetic methodologies based on C–H/C–[M],[9] C–H/C–X,[10] and C–H/C–H[11] coupling reactions were successfully developed. Among these synthetic approaches, connecting two substrates through twofold activation of unfunctionalized C–H bonds, so called cross-dehydrogenative couplings (CDC), is regarded as the most step-economical way to facilely extend the carbon chains.[12] Furthermore, in CDC type reactions, direct C_{sp2}–H/C_{sp2}–H coupling has been proved to be a viable synthetic tool to efficiently prolong the π-conjugated lengths/systems.[13] However, we noticed that by far the use of C_{sp2}–H/C_{sp2}–H (cross)coupling as key transformations to access π-functional oligo(hetero)aryls for optoelectronic applications is very rare.[14] In addition to You and coworkers describing a Rh(III)-catalyzed oxidative C–H/C–H reaction route to white light-emitting materials,[15] in 2017 our group reported a straightforward C_{sp2}–H/C_{sp2}–H cross-coupling strategy under Pd-catalysis for the rapid preparation of various D–A-π-A type small-molecular dyes, two of which were fabricated as dye-sensitized solar cells (DSSC), exhibiting the highest PCE of 4.85%.[16] When developing succinct new synthetic routes, we have also been searching for potentially useful π-conjugated building blocks with high-planarity which may facilitate electron/hole mobilities and eventually expect to improve the photon-to-current efficiencies while fabricated in photovoltaic devices. Recently, we found that naphtho[2,1-*b*:3,4-*b*′]dithiophene (NDT) was a popular candidate since it had been extensively investigated and employed either as organic light-emitting diode (OLED),[17] organic field-effect transistors (OFET),[18] organic solar cells (OSC),[19] or DSSC[20] due to its plain structure and uncomplicated synthesis with cost-effective starting materials. Nevertheless, in contrast to above diverse applications, there were only two articles describing the use of NDT core-based oligoaryls as hole-transporting material (HTM) for perovskite solar cells (PSC).[17,21] Itami published a naphtho[2,1-*b*:3,4-*b*′]dithiophene derivative which was fabricated as hole-transport layer in PSC, showing the PCE of 6.7%.[21] In the light of Itami's results and according to our previous publications regarding the π-spacer effect on the PCE improvement of HTM/PSC,[22] we anticipated that inserting appropriate π-spacers between the core- and end-group would substantially promote the electrical and photovoltaic performances of HTMs. Hence, instead of choosing the previously used 3,4-ethylenedioxythiophene (EDOT) as π-spacers, we intend to introduce a simpler alkene moiety between NDT and the end-group. Encouragingly, by inserting two additional olefin moieties into NDT core-based HTM as π-spacers, preliminary results of the relevant PSC devices displayed a significant progress in which the PCE was considerably improved from 6.7% to 17.2% (Figure 1).

Moreover, most of the HTM synthesis relied on Suzuki reactions or Migita-Kosugi-Stille couplings as key transformations, which required the prefunctionalization of both reaction

[a] *C.-C. Hsu,[+] X.-W. Wu, L. Lin, W.-L. Yu, Prof. Dr. C.-Y. Liu*
Department of Chemical and Materials Engineering
National Central University
Jhongli District, Taoyuan City 320, Taiwan
E-mail: cyliu0312@ncu.edu.tw
Homepage: http://www.en.cme.ncu.edu.tw/products_detail/101.htm
[b] *Prof. Dr. K.-M. Lee[+]*
Department of Chemical and Materials Engineering/Department of Pediatrics
Chang Gung University/Chang Gung Memorial Hospital
Guishan District, Taoyuan City 333, Taiwan
[c] *Prof. Dr. K.-M. Lee[+]*
College of Environment and Resources, Ming Chi University of Technology,
New Taipei City 243, Taiwan
[+] *These authors contributed equally to this work.*
Supporting information for this article is available on the WWW under https://doi.org/10.1002/chem.202302552

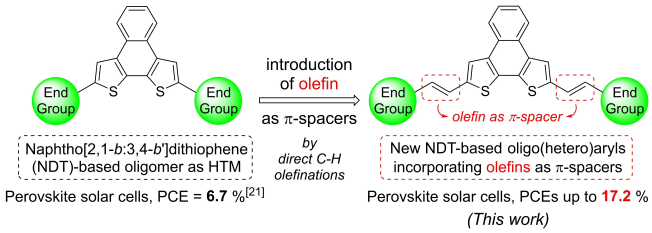

Figure 1. New NDT core-based HTMs incorporating additional olefins as π-spacers substantially improved the PCE of perovskite solar cells.

substrates including borylation, stannylation, and halogenations (Eq. 1., Scheme 1).[23] Recently, few HTM/PSCs-related papers avoided the preparation of organometallic reagents, directly coupling the C_{sp2}–H bond with C_{sp2}–X. This created a series of step-economical synthetic approaches for high-performance hole-transport small molecules (Eq. 2., Scheme 1).[24] Accordingly, we wish to challenge and examine the most succinct synthetic route to build HTM-oriented oligo(hetero)aryls by the straightforward C_{sp2}–H/C_{sp2}–H coupling reactions (Eq. 3., Scheme 1). To the best of our knowledge, no reports on the use of C_{sp2}–H/C_{sp2}–H cross-dehydrogenative couplings (direct C–H olefinations) in the design and rapid synthesis of hole-transporting molecules for PSCs have appeared to date.

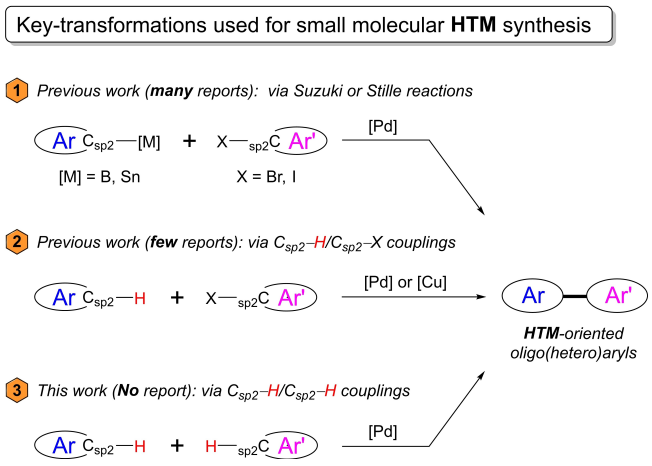

Scheme 1. Different synthetic routes to HTM-oriented oligo(hetero)aryls.

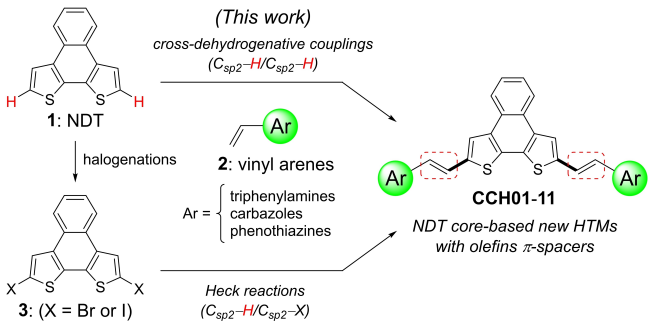

Scheme 2. Comparison of the key reactions to access NDT core-based new HTMs with olefin π-spacers: direct C–H olefinations *vs.* Heck reactions.

Results and Discussion

Firstly, as shown in Scheme 2, we demonstrated our synthetic plan that directly coupled **1** (naphtho[2,1-*b*:3,4-*b*′]dithiophene, NDT) with vinyl arenes **2** through Pd-catalyzed C_{sp2}–H/C_{sp2}–H cross-dehydrogenative couplings (CDC), affording various NDT core-based new HTMs incorporating alkenes as π-spacers (**CCH01**-**11**). Compared to using Heck reactions as key step, this synthetic approach based on direct C–H olefinations omitted the halogenation reactions (from **1** to **3**).

Next, in order to find the optimum reaction conditions, the direct C–H olefinations were examined by coupling NDT **1** with a commercially available 4-vinylanisole **2a** (Scheme 3). The data/results were detailed in Table S1 (Supporting Information, page S4–S5).

Initially, under a palladium catalysis using pyridine as base, a series of copper-based salts were investigated as essential oxidant, respectively, generating the desired product **CCH01** in 0–52% yields (entries 1–5). Compared to others, we noticed the inexpensive $Cu(OAc)_2$ gave a promising isolated yield of 52% (entry 1). From entries 6 through 11, a variety of silver salts were evaluated, and we were pleased to find the conditions with Ag_2CO_3 showed the highest conversion and afforded **CCH01** in 64% (entry 6). Relatively lower yields were observed with Ag_2O and AgOAc (33% and 38%, entries 7 and 8). Direct C–H olefinations of **1** using AgOTf, $AgSbF_6$, or AgF did not proceed at all and the starting materials were recovered (entries 9–11). Fe(III)-based complexes were also utilized as oxidants, however, **CCH01** was isolated in only trace quantities (entries 12–14). Further, MnO_2, $Mn(OAc)_2{\cdot}4H_2O$, or $K_2S_2O_8$ were examined individually under similar reaction conditions. It was found they were ineffective towards present C–H/C–H couplings (trace-16%, entries 15–17). Next, we fixed on the employment of Ag_2CO_3 to perform the optimization of bases. However, except DABCO shown in entry 21 (30%), the dehydrogenation hardly took place with DMAP, piperidine, or DBU (trace, entries 18–20). Finally, solvent screenings were conducted. The results indicated that other low-polarity solvents including toluene and 1,4-dioxane gave lower yields (29% and 30%, entries 22 and 23) while compared with *m*-xylene. Reactions in polar aprotic ones (DMAc, DMPU) did not make significant improvements (39% and 35%, entries 24 and 25). Two fluorine-containing protic solvents (TFE, HFIP) appeared to be inefficient for current CDC type reactions (0%, entries 26–27). Therefore, based on above considerations, we decided to use the optimized parameters acquired in entry 6, and tried a milder reaction condition (90 °C, 12 h) to see if a comparable yield would be obtained. However, a poor isolated yield of **CCH01**

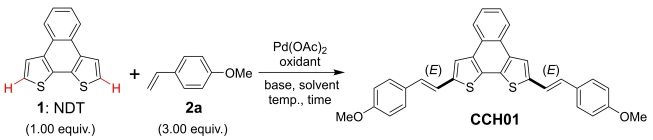

Scheme 3. Optimization of reaction conditions for the direct C_{sp2}–H/C_{sp2}–H couplings using NDT **1** and olefin **2a** as starting materials.

(12%, entry 28) implied the twofold C–H olefinations require a higher reaction temperature (125 °C) and a longer reaction time (24 h).

The reaction conditions shown in entry 6 were used to investigate the substrate scope of the twofold C–H olefinations by coupling of **1** (core-group) with a variety of vinyl arenes (end-groups: **2b–k**) (Table 1). **2b–k** are all HTM-oriented molecules consisting of electron-donating units such as triphenylamine (TPA), carbazole (Cbz), or phenothiazine (PTZ) derivatives. The substituents attached on **2b–k** were classified as methoxy (–OMe), *t*-butyl (*t*-Bu), and methoxy/(poly)fluoro-merged types. First, under optimum reaction parameters, direct C–H/C–H couplings of **1** took place with vinyl TPA (**2b**), vinyl Cbz (**2c**), or vinyl PTZ (**2d**), repectively, which afforded the desired products **CCH02-04** (41%, 60%, 18%). We speculated that the low isolated yield of **CCH04** might result from the instability of **2d**. During the preparation and purification processes whenever in solutions, we observed an instant color change from yellow to dark blue while **2d** was dissolved in dichloromethane or chloroform, presumably implying **2d** decomposed rapidly in its solution state. For the *t*-Bu substituted end-groups, we employed the derivatives of vinyl TPA (**2e**) and vinyl Cbz (**2f**) to examine the CDC reactions, which led to the formation of **CCH05-06** (71%, 25%). Furthermore, since the introduction of fluorine atoms onto small-molecule hole-transport materials has been shown to exhibit promising photovoltaic performances of PSC devices,[25] we hereby demonstrated a series of oligoheteroarenes bearing F- or CF_3-substituents on corresponding end-groups from **2g** through **2k**. By conducting direct C–H olefinations, new HTM molecules possessing (poly)fluoro moieties were facilely obtained (**CCH07-10**, 20–49%). Only trace amount of **CCH11** was isolated because this compound was fairly difficult to separate from a complex mixture. In general, **CCH04**, **CCH06**, **CCH08**, **CCH10**, and **CCH11** were produced along with a considerable quantity of undesired byproducts such as the homocoupled adducts from the corresponding end-group molecules and the mono-olefinated NDT (**1**). This made it more difficult for us to isolate the target HTMs, thus leading to the relatively lower yields of above compounds of interest. Besides, the direct C–H olefination of NDT exhibited high (*E*)-stereoselectivity since the formation of (*Z*)-isomers was hardly observed.

Next, we performed the measurements of optical, electrochemical, and thermal stability of **CCH01-10** and the results were collected in Table 2 and illustrated in Figure 2~7. Among these data, the HOMO energy level (E_{HOMO}) is representative since it indicates whether each HTM molecule could be efficiently extract holes from the perovskite layer ($CH_3NH_3PbI_3$) of PSC devices. The optimal HOMO energy of HTM is supposed to be located between the E_{HOMO} of perovskite layer (−5.43 eV) and silver electrode (−4.20 eV). **CCH03**, **CCH06**, and **CCH10** possessed relatively lower-lying E_{HOMO} (−5.53~−5.62 eV) than

Table 1. Investigation of substrate scope with respect to the vinyl arenes (**2b–k**).[a]

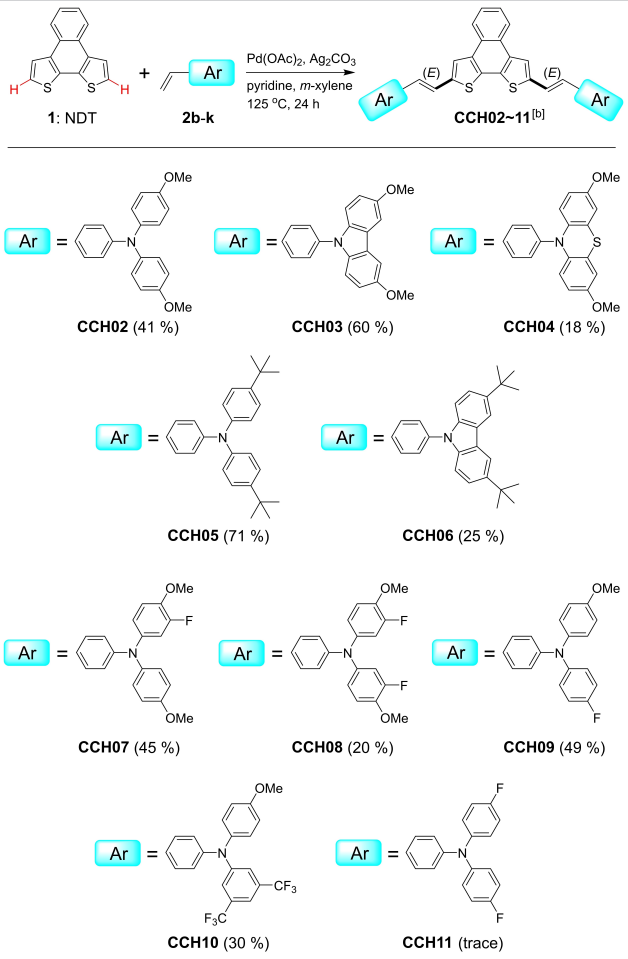

[a] Unless specified, the direct C–H olefinations were performed with **1** (0.5 mmol) and the corresponding vinyl arenes **2b–k** (1.5 mmol) respectively in the presence of $Pd(OAc)_2$ (10 mol%), Ag_2CO_3 (3.00 equiv.), and pyridine (3.00 equiv.) in *m*-xylene (1.0 mL) at 125 °C for 24 h.[b] Isolated yields.

Table 2. The optical, electrochemical, and thermal properties of **CCH01-10**.[a]

HTMs	ΔE_g^{opt} [eV][b]	E_{HOMO} [eV][c]	E_{LUMO} [eV][d]	T_d [°C][e]
CCH01	2.61	−5.41	−2.80	365
CCH02	2.37	−5.31	−2.94	326
CCH03	2.39	−5.53	−3.14	412
CCH04	2.41	−5.25	−2.84	398
CCH05	2.38	−5.37	−2.99	345
CCH06	2.57	−5.62	−3.05	415
CCH07	2.40	−5.36	−2.96	349
CCH08	2.43	−5.42	−2.99	331
CCH09	2.41	−5.38	−2.97	338
CCH10	2.50	−5.55	−3.05	295

[a] UV-Vis absorption and photoluminescence experiments were measured in dichloromethane solution. [b] ΔE_g^{opt} was calculated from the absorption onset of UV-Vis spectra, $\Delta E_g^{opt} = 1240/\lambda_{onset}$. [c] $E_{HOMO} = -(E_{ox,onset\ (vs.\ Fc/\ Fc^+)} + 5.16)$ eV. [d] $E_{LUMO} = E_{HOMO} + \Delta E_g^{opt}$. [e] T_d was obtained at 5% weight loss of HTMs.

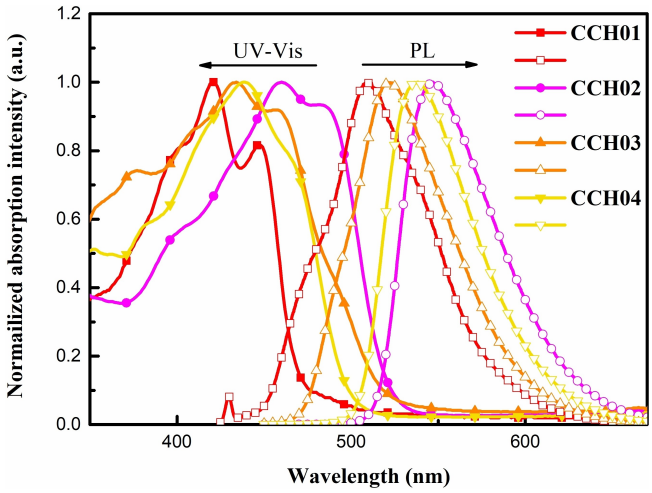

Figure 2. UV-Vis & photoluminescence spectra of **CCH01-04**.

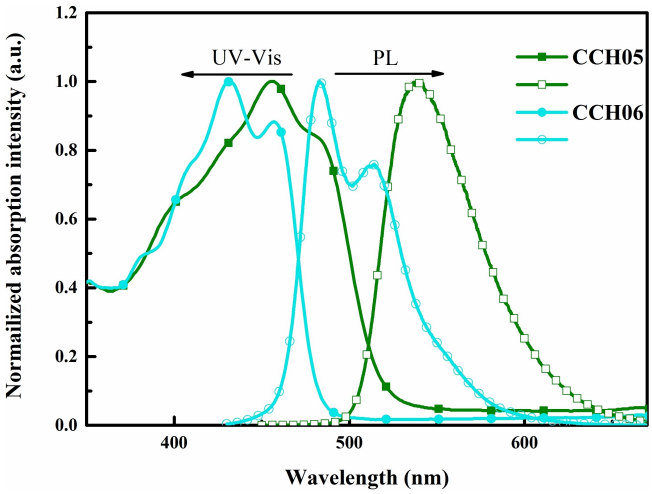

Figure 3. UV-Vis & photoluminescence spectra of **CCH05-06**.

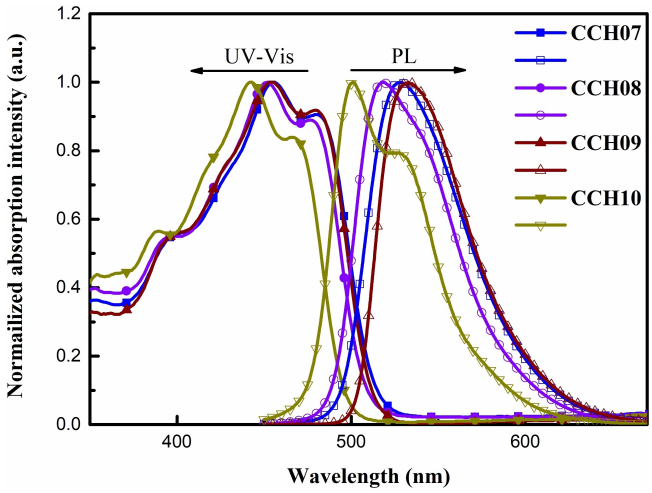

Figure 4. UV-Vis & photoluminescence spectra of **CCH07-10**.

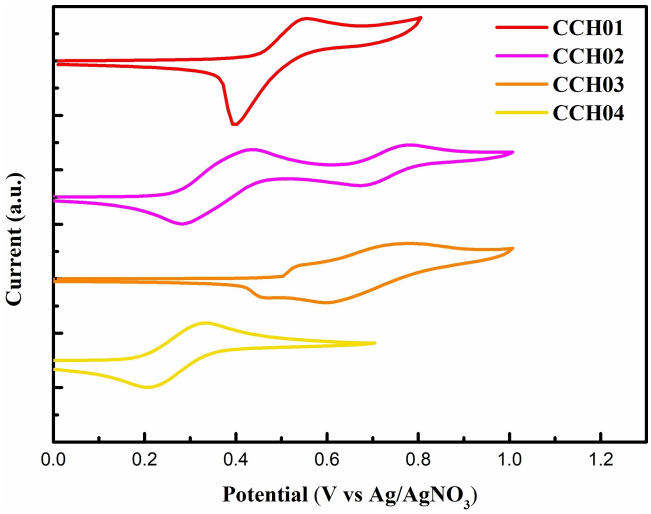

Figure 5. Cyclic voltammetry spectra of **CCH01-04**.

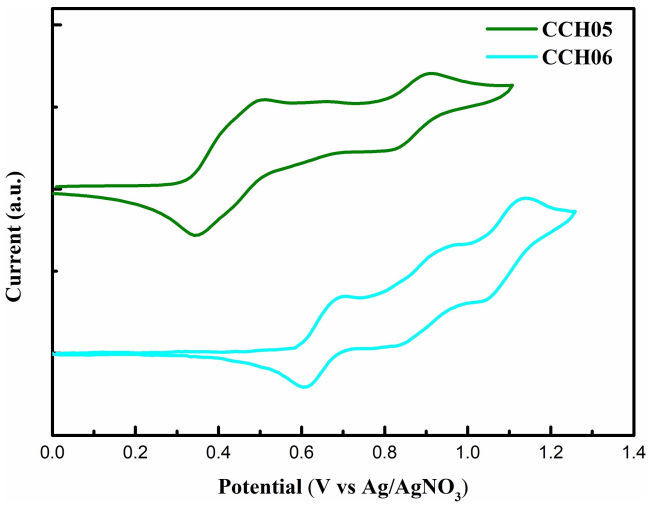

Figure 6. Cyclic voltammetry spectra of **CCH05-06**.

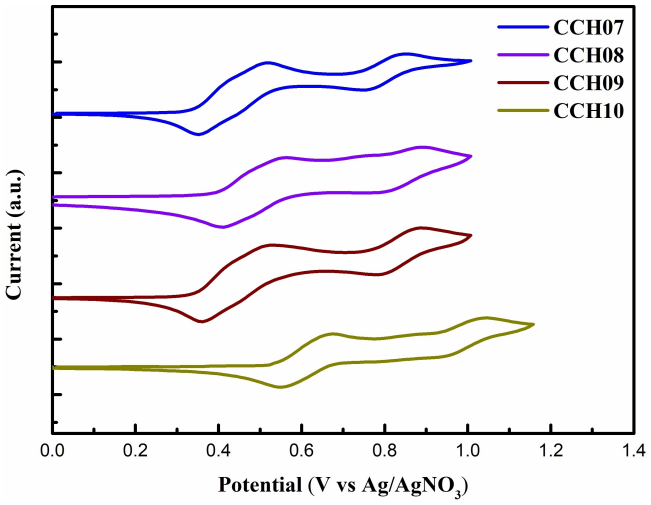

Figure 7. Cyclic voltammetry spectra of **CCH07-10**.

the perovskite layer, which implied that an inefficient hole-extraction would take place while these molecules are used as hole-transport layers. In addition, by performing the thermal gravimetric analysis (TGA), we found that **CCH03** and **CCH06** consisting of carbazole end-groups displayed superior decomposition temperatures (T_d = 412 and 415 °C).

The synthesized **CCH01**-**10** were then fabricated as hole-transport layer in perovskite-based solar devices, respectively, and the data of corresponding photovoltaic performances were summarized in Table 3. Devices with **spiro-OMeTAD** were utilized as reference cells (open-circuit voltage: V_{oc} = 1.07 V; short-circuit current: J_{sc} = 24.55 mA cm^{-2}; fill factor: FF = 73.30). Perovskite solar cells (PSC) with **CCH01** showed fairly low power conversion efficiency (PCE = 0.03 %). We found that the hole-transport layer of **CCH01**-based devices was somehow contaminated by the Ag electrode, thus causing the damage of whole spin-coated layers and resulting in the poorest PCE.[26] **CCH02** (dimethoxy-substituted triphenylamine)-based PSCs exhibited outstanding V_{oc} (1.04 V), J_{sc} (22.61 mA cm^{-2}), and FF (73.12), thus producing a promising PCE of 17.22 %. It was noteworthy that in this case no device oxidation process was needed and we observed an immediate 17.22 % PCE (**spiro-OMeTAD**-based PSCs usually required *at least* 12 hours of oxidation treatment to achieve high PCEs). However, devices with **CCH03** or **CCH04** demonstrated much lower PCEs (4.95 %, 1.03 %), presumably due to their poor solubility in spin-coating solvent (chlorobenzene) and leading to inferior film formation. Next, end-groups possessing *t*-butyl groups (**CCH05**&**06**) were examined. These PSCs also revealed low PCEs (3.33 %, 0.10 %). Furthermore, we investigated the HTMs of triphenylamine-based molecules bearing fluorine substituents (**CCH07**-**10**). Notably, PSCs with **CCH07** or **CCH08** led to promising PCEs (16.09 %, 15.11 %). Similar to the results acquired from **CCH02**, **CCH07**-based devices were able to display an immediate high PCE of 16.09 % without any oxidation process. However, **CCH09** and **CCH10** with fewer –OMe groups gave unsatisfactory results (PCE = 0.65~3.26 %). This indicated that, for current naphthodithiophene-based oligoaryls, the presence and quantity of methoxy groups constituted an important requirement in designing effective small-molecule organic HTMs.[27]

The photovoltaic performance of perovskite solar cells with **CCH01**-**10** was also presented by means of the diagram of photocurrent density-voltage (*J*-*V*) curves (Figure 8~10). The synthesized HTMs were classified according to the substituents on end-group molecules: **CCH01**-**04** with methoxy groups, **CCH05**-**06** with *t*-butyl groups, and **CCH07**-**10** with methoxy and fluoro groups. **CCH02**-based PSCs showed superior *J*-*V* values that are comparable to those of **spiro-OMeTAD**-based devices (Figure 8). PSCs with **CCH07**&**08** exhibited exceptional V_{oc} of 1.06–1.07 V which is nearly identical to the V_{oc} of devices using **spiro-OMeTAD** as HTM (Figure 10).

Finally, for the devices displaying higher PCEs (15.11~17.22 %), we focused on three corresponding HTMs (**CCH02**, **07**, and **08**) to further examine their hole-extraction abilities. This was realized by the measurement of steady-state photoluminescence (PL) and time-resolved photoluminescence (TRPL) of the devices fabricated in the configuration of glass/perovskite/HTMs. Spectra provided in Figure 11 revealed that

Table 3. Photovoltaic performance evaluation of the perovskite solar cells using **CCH01-10** as HTMs.[a,b]

HTMs		V_{oc} [V]	J_{sc} [mAcm^{-2}]	FF [%]	PCE [%]
CCH01	best	0.03	4.45	25.31	0.03
	average	0.03 ± 0.01	2.71 ± 0.85	25.44 ± 1.30	0.02 ± 0.01
CCH02	best	1.04	22.61	73.12	**17.22**
	average	1.00 ± 0.03	22.42 ± 0.36	66.66 ± 4.48	15.02 ± 1.52
CCH03	best	0.98	12.69	40.19	4.95
	average	0.99 ± 0.05	11.15 ± 1.16	34.66 ± 4.04	3.8 ± 0.73
CCH04	best	0.95	3.70	29.34	1.03
	average	0.87 ± 0.12	3.92 ± 0.61	31.52 ± 4.32	1.06 ± 0.17
CCH05	best	1.00	12.57	26.46	3.33
	average	0.95 ± 0.07	10.35 ± 1.64	23.91 ± 2.13	2.37 ± 0.61
CCH06	best	0.95	0.40	27.09	0.10
	average	0.67 ± 0.32	0.4 ± 0.10	27 ± 7.56	0.07 ± 0.04
CCH07	best	1.06	22.81	66.86	**16.09**
	average	1.05 ± 0.02	21.85 ± 1.04	62.77 ± 2.86	14.46 ± 1.30
CCH08	best	1.07	21.82	64.56	**15.11**
	average	1.07 ± 0.02	21.95 ± 0.21	52.84 ± 5.46	12.44 ± 1.21
CCH09	best	0.99	10.86	30.27	3.26
	average	0.83 ± 0.27	10.39 ± 1.27	32.64 ± 10.92	2.58 ± 0.61
CCH10	best	0.42	4.78	32.06	0.65
	average	0.34 ± 0.13	4.28 ± 0.49	28.86 ± 2.31	0.43 ± 0.20
spiro-OMeTAD	best	1.07	24.55	73.30	**18.89**
	average	1.06 ± 0.01	24.03 ± 0.33	73.84 ± 1.05	18.4 ± 0.32

[a] Above statistical data were calculated based on 6–8 cells.
[b] Reverse scans.

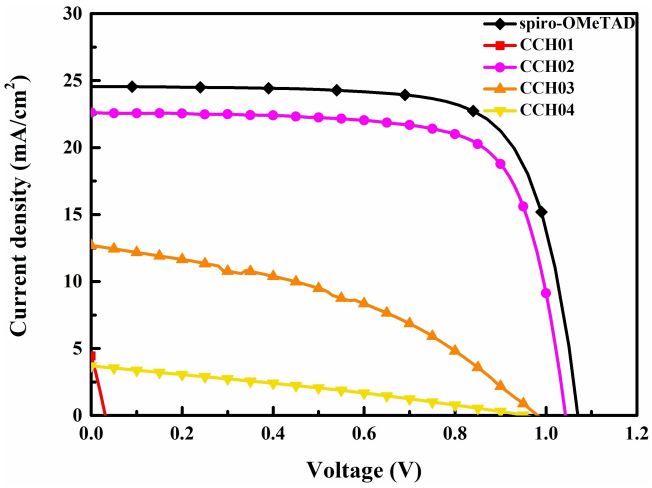

Figure 8. Photocurrent density-voltage (*J-V*) curves of perovskite solar cells using **CCH01-04** as HTMs.

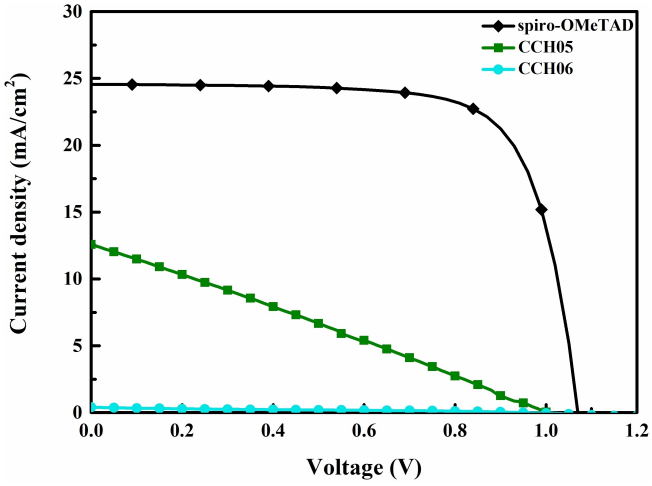

Figure 9. Photocurrent density-voltage (*J-V*) curves of perovskite solar cells using **CCH05-06** as HTMs.

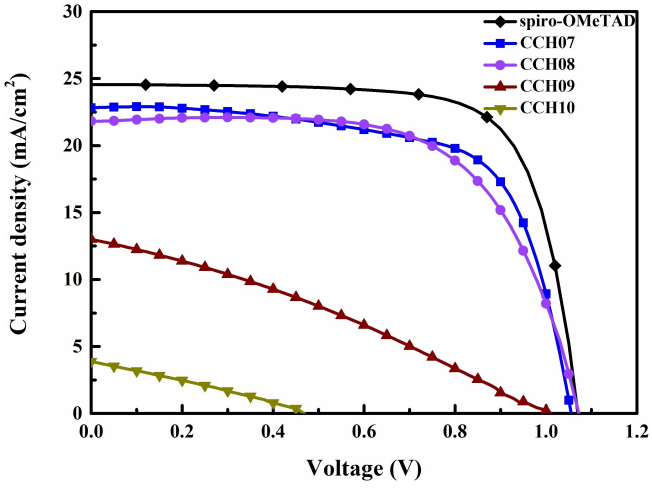

Figure 10. Photocurrent density-voltage (*J-V*) curves of perovskite solar cells using **CCH07-10** as HTMs.

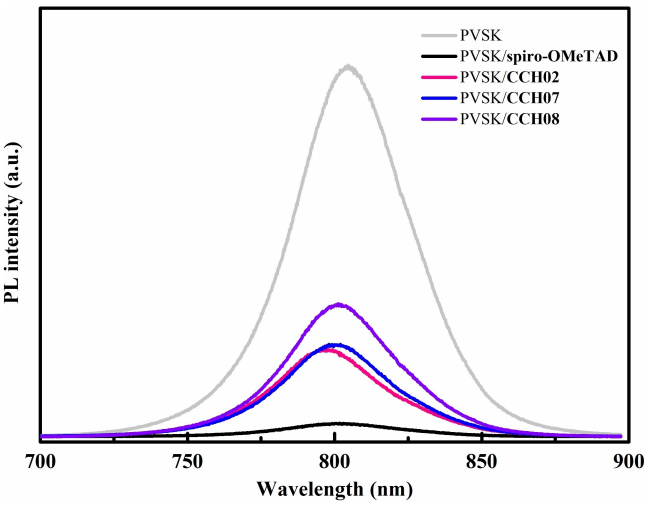

Figure 11. Steady-state PL spectra of the devices fabricated as glass/perovskite/HTM(**CCH02**, **07**, or **08**).

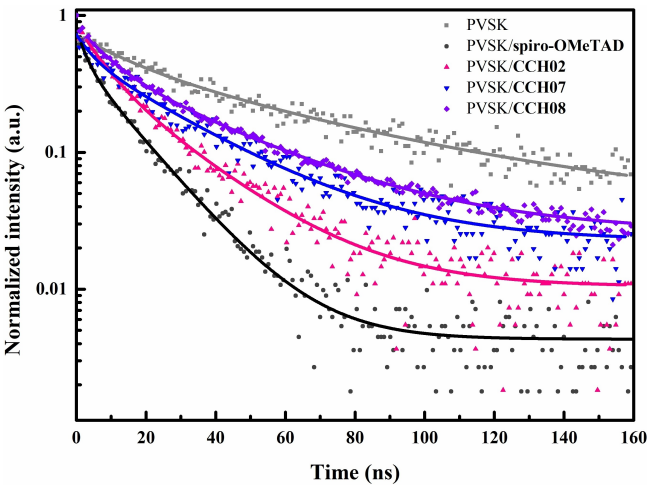

Figure 12. Time-resolved PL spectra of the devices fabricated as glass/perovskite/HTM(**CCH02**, **07**, or **08**).

CCH02- and **CCH07**-based devices exhibited comparable PL quenching effects, which is stronger than that of the devices with **CCH08**. This indicated **CCH02**&**07** had superior capability of extracting holes at the interface between perovskite- and hole transport-layers. In addition, the TRPL spectra given in Figure 12 demonstrated perovskite/**CCH02** possessed a relatively shorter average lifetime ($\tau_{average}$ = 10 ns; $\tau_{average}$ = 14 ns for perovskite/**CCH07**; $\tau_{average}$ = 15 ns for perovskite/**CCH08**), implying that **CCH02** could efficiently inhibited the recombination of electrons and holes generated from the photoactive perovskite-layer.

Conclusions

In summary, the most atom-economical cross-dehydrogenative coupling synthetic strategy involving the activation of two unfunctionalized C–H bonds has been applied in the facile

preparation of new hole-transporting materials for the first time. Hence, direct C–H olefination reactions of naphtho[2,1-*b*:3,4-*b'*]dithiophene (NDT) were optimized by screening key reaction parameters including oxidants, bases and solvents, affording **CCH01-10** with olefin π-spacers in 18–71% isolated yields. Three of the obtained HTMs (**CCH02**, **07**, and **08**) exhibited promising PCEs exceeding 15% while fabricated as the hole-transport layer in corresponding perovskite solar cells. Among them, **CCH02**&**07**-based PSCs were capable of displaying over 16% PCEs without any device oxidation treatment. In contrast, the most popular and commercially available HTM, **spiro-OMeTAD**, required at least 12-hour oxidation to achieve the highest PCE. This work successfully bridged the most succinct while challenging C_{sp2}–H/C_{sp2}–H coupling approach in synthetic chemistry with HTMs/PSCs in the field of organic optoelectronic materials.

Experimental Section

General Procedure for the synthesis of **CCH02**: To a solution of $Pd(OAc)_2$ (12 mg, 10 mol%), Ag_2CO_3 (414 mg, 3.00 equiv.), and pyridine (119 mg, 3.00 equiv.) in *m*-xylene (1.0 mL) in a heat-gun dried sealed tube were added naphtho[2,1-*b*:3,4-*b'*]dithiophene (**1**) (120 mg, 0.50 mmol) and the corresponding vinyl arene (**2b**) (497 mg, 1.50 mmol) under N_2. The reaction mixture was then heated at 125 °C under N_2 for 24 h. After the reaction mixture had cooled to room temperature, water (10 mL) was added. The mixture was extracted with ethyl acetate (2×20 mL), and the combined organic layers were washed with brine (50 mL), dried (Na_2SO_4) and concentrated in *vacuo*. Purification by column chromatography (ethyl acetate:hexanes = 15:85) gave the desired product **CCH02** (184 mg, 41%, brown solid).

Supporting Information

The authors have cited additional references within the Supporting Information.[28–33]

Acknowledgements

Financial support provided by the Ministry of Science and Technology (MOST), Taiwan (MOST 111-2113-M-008-008 and 108-2628-E-182-003-MY3), National Central University (NCU), Chang Gung University (QZRPD181) and Chang Gung Memorial Hospital, Linkou, Taiwan (CMRPD2M0041) are gratefully acknowledged. We also thank the instrument center (R&D office, NCU, MOST 110–2731-M-008-001) for the technical support of NMR and mass analysis.

Conflict of Interests

The authors declare no conflict of interest.

Data Availability Statement

The data that support the findings of this study are available in the supplementary material of this article.

Keywords: Direct C–H Olefination · Hole-Transporting Material · Naphthodithiophene · Perovskite Solar Cell · Synthesis Design

[1] S. Murai, F. Kakiuchi, S. Sekine, Y. Tanaka, A. Kamatani, M. Sonoda, N. Chatani, *Nature* **1993**, *366*, 529.
[2] F. Kakiuchi, N. Chatani, *Adv. Synth. Catal.* **2003**, *345*, 1077.
[3] D. Alberico, M. E. Scott, M. Lautens, *Chem. Rev.* **2007**, *107*, 174.
[4] P. Gandeepan, T. Müller, D. Zell, G. Cera, S. Warratz, L. Ackermann, *Chem. Rev.* **2019**, *119*, 2192.
[5] a) Y. Segawa, T. Maekawa, K. Itami, *Angew. Chem. Int. Ed.* **2015**, *54*, 66; b) J. Yamaguchi, A. D. Yamaguchi, K. Itami, *Angew. Chem. Int. Ed.* **2012**, *51*, 8960.
[6] a) H. Saito, K. Yamamoto, Y. Sumiya, L.-J. Liu, K. Nogi, S. Maeda, H. Yorimitsu, *Chem. Asian J.* **2020**, *15*, 2442; b) T. Yanagi, K. Nogi, H. Yorimitsu, *Tetrahedron Lett.* **2018**, *59*, 2951.
[7] J. He, M. Wasa, K. S. L. Chan, Q. Shao, J.-Q. Yu, *Chem. Rev.* **2017**, *117*, 8754.
[8] T. W. Lyons, M. S. Sanford, *Chem. Rev.* **2010**, *110*, 1147.
[9] L. Ackermann, R. Vicente, A. R. Kapdi, *Angew. Chem. Int. Ed.* **2009**, *48*, 9792.
[10] a) B. Liégault, D. Lapointe, L. Caron, A. Vlassova, K. Fagnou, *J. Org. Chem.* **2009**, *74*, 1826; b) R. Matsidik, J. Martin, S. Schmidt, J. Obermayer, F. Lombeck, F. Nübling, H. Komber, D. Fazzi, M. Sommer, *J. Org. Chem.* **2015**, *80*, 980; c) A. Nitti, M. Signorile, M. Boiocchi, G. Bianchi, R. Po, D. Pasini, *J. Org. Chem.* **2016**, *81*, 11035; d) A. Nitti, G. Bianchi, R. Po, T. M. Swager, D. Pasini, *J. Am. Chem. Soc.* **2017**, *139*, 8788; e) P.-A. Sommai, S. Tetsuya, K. Yoshiki, M. Masahiro, N. Masakatsu, *Bull. Chem. Soc. Jpn.* **1998**, *71*, 467.
[11] a) Y. Fujiwara, O. Maruyama, M. Yoshidomi, H. Taniguchi, *J. Org. Chem.* **1981**, *46*, 851; b) C.-J. Li, *Acc. Chem. Res.* **2009**, *42*, 335; c) C. Liu, H. Zhang, W. Shi, A. Lei, *Chem. Rev.* **2011**, *111*, 1780.
[12] a) C.-Y. Huang, H. Kang, J. Li, C.-J. Li, *J. Org. Chem.* **2019**, *84*, 12705; b) C. S. Yeung, V. M. Dong, *Chem. Rev.* **2011**, *111*, 1215.
[13] C. Liu, J. Yuan, M. Gao, S. Tang, W. Li, R. Shi, A. Lei, *Chem. Rev.* **2015**, *115*, 12138.
[14] A. Mori, A. Sugie, *Bull. Chem. Soc. Jpn.* **2008**, *81*, 548.
[15] B. Li, J. Lan, D. Wu, J. You, *Angew. Chem. Int. Ed.* **2015**, *54*, 14008.
[16] Y.-S. Ciou, P.-H. Lin, W.-M. Li, K.-M. Lee, C.-Y. Liu, *J. Org. Chem.* **2017**, *82*, 3538.
[17] H. D. Pham, H. Hu, F.-L. Wong, C.-S. Lee, W.-C. Chen, K. Feron, S. Manzhos, H. Wang, N. Motta, Y. M. Lam, P. Sonar, *J. Mater. Chem. C* **2018**, *6*, 9017.
[18] a) I. Osaka, S. Shinamura, T. Abea, K. Takimiya, *J. Mater. Chem. C* **2013**, *1*, 1297; b) K. Zhang, J. Zhang, X. Zhang, G. Yu, M. S. Wong, *Tetrahedron Lett.* **2018**, *59*, 641.
[19] a) M. Löbert, A. Mishra, C. Ulrich, M. Pfeiffer, P. Bäuerle, *J. Mater. Chem. C* **2014**, *2*, 4879; b) J. Zhu, Z. Ke, Q. Zhang, J. Wang, S. Dai, Y. Wu, Y. Xu, Y. Lin, W. Ma, W. You, X. Zhan, *Adv. Mater.* **2018**, *30*, 1704713.
[20] X. Wang, L. Guo, P. F. Xia, F. Zheng, M. S. Wong, Z. Zhu, *J. Mater. Chem. A* **2013**, *1*, 13328.
[21] H.-A. Lin, N. Mitoma, L. Meng, Y. Segawa, A. Wakamiya, K. Itami, *Mater. Chem. Front.* **2018**, *2*, 275.
[22] a) Y.-K. Peng, K.-M. Lee, C.-C. Ting, M.-W. Hsu, C.-Y. Liu, *J. Mater. Chem. A* **2019**, *7*, 24765; b) L. Lin, C.-C. Hsu, K.-M. Lee, W.-L. Yu, M.-Y. Lin, C.-Y. Liu, *ChemistrySelect* **2022**, *7*, e202202472; c) C.-H. Tu, K.-M. Lee, J.-H. Chen, C.-H. Chiang, S.-C. Hsu, M.-W. Hsu, C.-Y. Liu, *Org. Chem. Front.* **2022**, *9*, 2821; d) P.-H. Lin, K.-M. Lee, C.-C. Ting, C.-Y. Liu, *J. Mater. Chem. A* **2019**, *7*, 5934.
[23] a) H. Choi, H. M. Ko, J. Ko, *Dyes Pigm.* **2016**, *126*, 179; b) A. M. Ontoria, I. Zimmermann, I. G. Benito, P. Gratia, C. R. Carmona, S. Aghazada, M. Grätzel, M. K. Nazeeruddin, N. Martín, *Angew. Chem. Int. Ed.* **2016**, *55*, 6270.
[24] a) C. Lu, M. Paramasivam, K. Park, C. H. Kim, H. K. Kim, *ACS Appl. Mater. Interfaces* **2019**, *11*, 14011; b) Y.-C. Chang, K.-M. Lee, C.-H. Lai, C.-Y. Liu, *Chem. Asian J.* **2018**, *13*, 1510; c) J.-H. Chen, K.-M. Lee, C.-C. Ting, C.-Y. Liu, *RSC Adv.* **2021**, *11*, 8879; d) Y.-C. Chang, K.-M. Lee, C.-C. Ting, C.-Y. Liu, *Mater. Chem. Front.* **2019**, *3*, 2041; e) K.-M. Lu, K.-M. Lee, C.-H. Lai, C.-

C. Ting, C.-Y. Liu, *Chem. Commun.* **2018**, *54*, 11495; f) C.-Y. Liu, P.-H. Lin, K.-M. Lee, *Chem. Rec.* **2021**, *21*, 1.
[25] a) M. Jeong, I. W. Choi, E. M. Go, Y. Cho, M. Kim, B. Lee, S. Jeong, Y. Jo, H. W. Choi, J. Lee, J.-H. Bae, S. K. Kwak, D. S. Kim, C. Yang, *Science* **2020**, *369*, 1615; b) L. Wan, W. Zhang, S. Fu, L. Chen, Y. Wang, Z. Xue, Y. Tao, W. Zhang, W. Song, J. Fang, *J. Mater. Chem. A* **2020**, *8*, 6517; c) Y. K. Wang, H. Ma, Q. Chen, Q. Sun, Z. Liu, Z. Sun, X. Jia, Y. Zhu, S. Zhang, J. Zhang, N. Yuan, J. Ding, Y. Zhou, B. Song, Y. Li, *ACS Appl. Mater. Interfaces* **2021**, *13*, 7705.
[26] Y. Kato, L. K. Ono, M. V. Lee, S. Wang, S. R. Raga, Y. Qi, *Adv. Mater. Interfaces* **2015**, *2*, 1500195.
[27] S. Lee, J. Lee, H. Park, J. Choi, H. W. Baac, S. Park, H. J. Park, *ACS Appl. Mater. Interfaces* **2020**, *12*, 40310.
[28] B. Rungtaweevoranit, A. Butsuri, K. Wongma, K. Sadorn, K. Neranon, C. Nerungsi, T. Thongpanchang, *Tetrahedron Lett.* **2012**, *53*, 1816.
[29] S. Barlow, C. Risko, S.-J. Chung, N. M. Tucker, V. Coropceanu, S. C. Jones, Z. Levi, J.-L. Brédas, S. R. Marder, *J. Am. Chem. Soc.* **2005**, *127*, 16900.
[30] K. Araki, X. P. Qiu, JP Patent 2002097181, **2002**.
[31] J. C. Warner, Patent WO2018208709, **2018**.
[32] M. V. Nandakumar, J. G. Verkade, *Tetrahedron* **2005**, *61*, 9775.
[33] R. Schroot, C. Friebe, E. Altuntas, S. Crotty, M. Jager, U. S. Schubert, *Macromolecules* **2013**, *46*, 2039.

Manuscript received: August 5, 2023
Accepted manuscript online: November 23, 2023
Version of record online: ■■, ■■

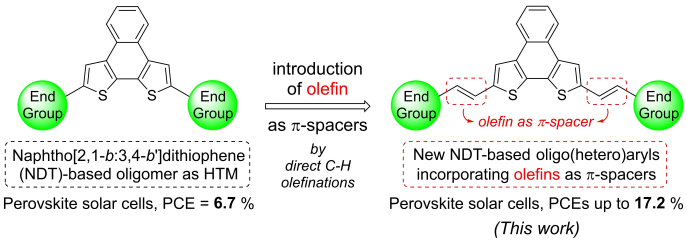

For the first time, C–H/C–H cross-dehydrogenative couplings (direct C–H olefinations) are used as key step to access small-molecule hole-transporting materials (HTMs). NDT core-based HTMs incorporating additional olefins as π-spacers substantially improve the PCE of perovskite solar cells of up to 17.2 %.

*C.-C. Hsu, Prof. Dr. K.-M. Lee, X.-W. Wu, L. Lin, W.-L. Yu, Prof. Dr. C.-Y. Liu**